

Moiré-driven multiferroic order in twisted CrCl₃, CrBr₃ and CrI₃ bilayers

Adolfo O. Fumega¹ and Jose L. Lado¹

¹*Department of Applied Physics, Aalto University, 02150 Espoo, Finland*

Layered van der Waals materials have risen as a powerful platform to engineer artificial competing states of matter. Here we show the emergence of multiferroic order in twisted chromium trihalide bilayers, an order fully driven by the moiré pattern and absent in aligned multilayers. Using a combination of spin models and ab initio calculations, we show that a spin texture is generated in the moiré supercell of the twisted system as a consequence of the competition between stacking-dependent interlayer magnetic exchange and magnetic anisotropy. An electric polarization arises associated with such a non-collinear magnetic state due to the spin-orbit coupling, leading to the emergence of a local ferroelectric order following the moiré. Among the stoichiometric trihalides, our results show that twisted CrBr₃ bilayers give rise to the strongest multiferroic order. We further show the emergence of a strong magnetoelectric coupling, which allows the electric generation and control of magnetic skyrmions. Our results put forward twisted chromium trihalide bilayers, and in particular CrBr₃ bilayers, as a powerful platform to engineer artificial multiferroic materials and electrically tunable topological magnetic textures.

I. INTRODUCTION

Multiferroic materials display more than one ferroic order at the same time^{1–3}, and in particular, they can simultaneously host magnetic and ferroelectric orders. The existence of multiple symmetry-breaking orders allows having a coupling between electric and magnetic degrees of freedom⁴. Over the last two decades, a variety of multiferroic bulk compounds has been demonstrated^{5–8}, providing alternative strategies for multifunctional devices^{7,9}. However, focusing on the realm of two-dimensional (2D) materials, purely 2D multiferroics have remained elusive until the recent demonstration of multiferroic order in Ni₂^{10,11}. Beyond isolating individual multiferroic monolayers, a potential alternative strategy to realize multiferroic order in van der Waals materials relies on artificially engineering it from originally non-multiferroic monolayers¹². The electric control of magnetism provided by van der Waals multiferroics would open radically new ways of controlling artificial van der Waals matter^{13–25}.

The weak bonding between layers in van der Waals materials allows combining monolayers in twisted heterostructures. Monolayer 2D materials can display different symmetry-breaking orders^{11,26–28}, constituting a family of minimal building blocks that can be used to artificially engineer other emergent orders. This strategy has been widely exploited to engineer moiré correlated and topological states using 2D materials^{13,16,17,29–33}. Recently, this strategy has been extended to 2D magnetic materials including chromium trihalides, leading to a variety of twist-induced magnetic orders^{34–41}. However, using twist engineering to realize a multiferroic order has so far remained unexplored.

Here we demonstrate the emergence of a multiferroic state in the family of twisted chromium trihalide CrX₃ (X=Cl, Br and I) bilayers by combining first principles and effective spin Hamiltonians. We first show the emergence of a non-collinear spin texture due to the modulation of the interlayer exchange coupling in the moiré

unit cell. Associated with the spin texture an electric polarization emerges as a consequence of spin-orbit coupling (SOC) and the local magnetic non-collinearity in the moiré domains. Using ab initio calculations we extract the value of the electric polarization driven by non-collinear magnetic texture, and demonstrate its dependence on the halide of CrX₃. Therefore, we provide a quantification of the resulting multiferroic order. Furthermore, we analyze the emergent magnetoelectric coupling, demonstrating how it allows us to electrically drive transitions between different topological spin textures employing an interlayer bias.

II. RESULTS AND DISCUSSION

We start our analysis by describing the magnetic order that emerges in twisted CrX₃ bilayers. The magnetic behavior of CrX₃ monolayers can be described by a spin Hamiltonian in a honeycomb lattice

$$\mathcal{H} = -\frac{J}{2} \sum_{\langle i,j \rangle} \mathbf{S}_i \cdot \mathbf{S}_j - \frac{A_v}{2} \sum_{\langle i,j \rangle} S_i^z S_j^z - A_u \sum_i (S_i^z)^2 + \mathcal{V}, \quad (1)$$

where J is the first neighbor intralayer ferromagnetic exchange, taking a value on the order of 2–3 meV^{42–44}. A_v is the anisotropic magnetic exchange. A_u is the single-ion anisotropy, which is dominated by A_v in CrI₃, CrBr₃, and competing with A_v in CrCl₃⁴⁵. Our analysis will focus on the anisotropy regime leading to out-of-plane easy axis, that corresponds to CrI₃, CrBr₃ and slightly strained CrCl₃^{46,47}. The term \mathcal{V} contains additional contributions that do not qualitatively affect our analysis, including Kitaev exchange⁴⁸, biquadratic exchange⁴⁹, direct Dzyaloshinskii-Moriya interaction⁵⁰, and dipolar coupling⁵¹.

Considering now two layers of CrX₃ stacked together an interlayer magnetic exchange J_M will arise. A moiré pattern like the one shown in Fig. 1a emerges for twist

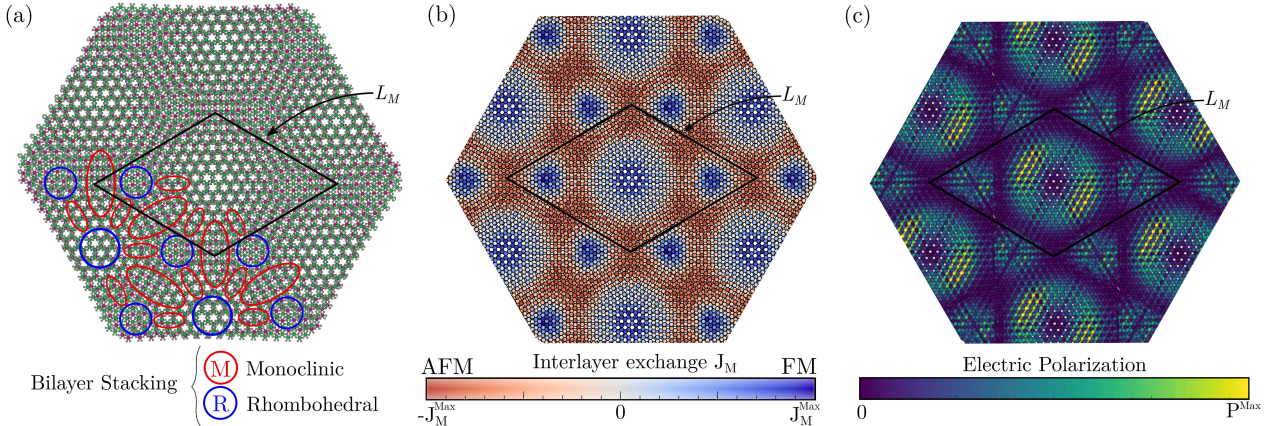


FIG. 1. (a) Top view of the twisted CrX₃ bilayer at small angles. Ligand atoms X are represented in gray, and Cr atoms of the bottom (top) layer in pink (green). The moiré unit cell is described by a lattice parameter of the moiré length scale L_M . The emergent moiré pattern leads to regions with monoclinic (M) and rhombohedral (R) stackings, highlighted in red and blue respectively. (b) Moiré profile for the interlayer magnetic exchange J_M originated from the different stackings. The interlayer magnetic exchange interaction is antiferromagnetic (ferromagnetic) in the monoclinic (rhombohedral) stacking. (c) Module of the local electric polarization associated with the moiré ground state spin texture.

angles lower than 3°. Depending on the stacking between layers two different regions can be distinguished, monoclinic and rhombohedral. Associated with these different regions the sign of J_M will change, i.e., J_M is ferromagnetic (positive) in the rhombohedral stacking and antiferromagnetic (negative) in the monoclinic one^{52–55}. This leads to a modulation of J_M in the moiré supercell like the one shown in Fig. 1b^{34–37,56,57}. Therefore, to model the twisted CrX₃ bilayer we add the interlayer interaction to the Hamiltonian of Eq. (1) as

$$\mathcal{H}_{Inter} = -\frac{1}{2} \sum_{i,j} J_M(\mathbf{r}_i, \mathbf{r}_j) \mathbf{S}_i \cdot \mathbf{S}_j, \quad (2)$$

where $J_M(\mathbf{r}_i, \mathbf{r}_j)$ is the site-dependent interlayer exchange⁵⁸. Since CrX₃ is composed of Cr³⁺ with a spin state S=3/2, we can solve in a classical way the spin Hamiltonian for the twisted system⁵⁹. The ground state magnetic order is depicted in Fig. 2a. We can see that a non-collinear magnetic texture emerges between ferromagnetic and antiferromagnetic regions in agreement with previous theoretical^{38,39} and experimental results^{34–37,40,41}. Taking this as the starting point, we now show that in the presence of spin-orbit coupling, this topologically-trivial spin texture leads to the emergence of an electric polarization \mathbf{P}_{ij} between first-neighbor spins in the same layer separated by a distance \mathbf{r}_{ij} due to the inverse Dzyaloshinskii-Moriya (DM) mechanism^{60,61}

$$\mathbf{P}_{ij} = \alpha \lambda_{SOC} (\mathbf{r}_{ij} \times (\mathbf{S}_i \times \mathbf{S}_j)), \quad (3)$$

where λ_{SOC} is a coefficient that controls the strength of the spin-orbit coupling and α is a proportionality constant that depends on the electronic structure and crystal environment, which is similar for the three chromium

trihalides. The polarization emerges at the middle point between the two neighboring spins \mathbf{S}_i and \mathbf{S}_j . From Eq. (3) we can clearly see the requirement of non-collinearity and the presence of SOC to produce an electric polarization. For the emerging ground state spin texture of the twisted system (Fig. 2a), the associated electric polarization when SOC is introduced is shown in Fig. 2b, with P_z the dominant component. From Figs. 2ab, we can observe that an electric polarization emerges in both layers in the areas where the non-collinear spin texture occurs. The polarization emerges locally, and for the ground state spin texture the net electric polarization is zero. Therefore, to analyze the strength of the multiferroic order as a function of the parameters that appear in the spin Hamiltonian, we will consider an average of the electric polarization module \bar{P} . The module of the electric polarization in the moiré system associated with the ground state spin texture can be seen in Fig. 1c. We can observe there, that the ground state breaks the C₆ symmetry of the original system leading to a C₂ symmetry. The lifted C₆ symmetry stems from a spontaneous symmetry breaking of the ground state due to the ratio between the parameters entering the spin Hamiltonian, analogous to the symmetry breaking associate to stripy magnetic orders. Figure 2c shows the average polarization as a function of the maximum interlayer exchange J_M^{max} . At low values, the twisted system behaves like two independent layers, remaining ferromagnetic, no spin texture emerges and consequently, there is no electric polarization. By increasing the interlayer coupling, non-collinearity appears and with it an associated electric polarization in virtue of Eq. (3). Figure 2d shows the average polarization as a function of the anisotropic exchange A_v . At high values, the twisted system tends to align the magnetic moments out of the plane. Therefore, no spin texture occurs and thus there is no electric

polarization. This situation happens for $A_v/J > 0.1$, so CrI₃ would be on the verge of displaying a multiferroic behavior due to its strong uniaxial anisotropy⁴⁵.

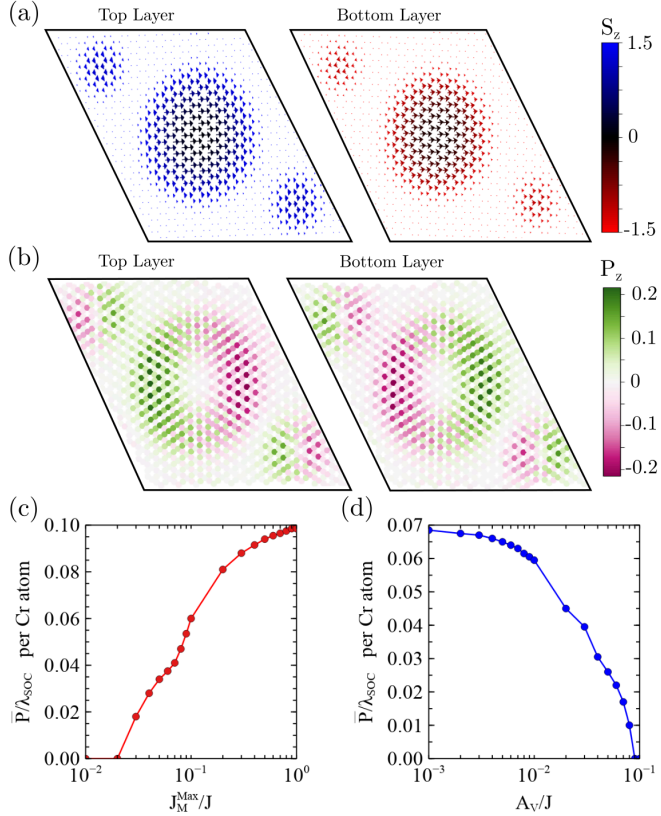


FIG. 2. Ground state solution of the spin Hamiltonian for the twisted system. (a) Ground state spin texture on the top (bottom) layer is shown in the left (right) panel. S_x and S_y components are depicted as a vector field. The color of the vectors shows the S_z component. (b) Associated electric polarization (P_z component) to the ground state magnetic texture. (c) Electric polarization average of the ground state as a function of the interlayer exchange maximum J_M^{\max} ($A_v/J = 0.01$ and $A_u/J = 0.001$). At low values of J_M^{\max} no spin texture is formed. (d) Electric polarization average of the ground state as a function of the anisotropic magnetic exchange A_v ($J_M^{\max}/J = 0.1$ and $A_u/J = 0.001$). At high values of A_v no spin texture is formed.

We now demonstrate and quantify, using density functional theory calculations⁶², the emergent electric polarization that we have seen that appears in the non-collinear moiré system in virtue of eq. (3). Performing first-principles calculations in a full twisted CrX₃ bilayer with spin-orbit coupling and non-collinear magnetism is well beyond the current computational capabilities. However, since the electric polarization arises locally, the ab initio analysis can be performed in a system like the one shown in Fig. 3a by imposing a magnetic texture in the CrX₃ layer like the one shown in Fig. 3b, that resembles the kind of spin texture found in the ground state between rhombohedral and monoclinic regions. We set the same out-of-plane spin texture

to the three compounds to systematically extract the effect of the halide atom and quantification of the inverse DM interaction⁶³. The associated polarization of a non-collinear texture given in eq. (3) can be rewritten in terms of a spin spiral propagation vector \mathbf{q} and the spin rotation axis $\mathbf{e} = (0, -1, 0)$, leading to an electric polarization of the spin texture^{60,61}

$$\mathbf{P} = \beta \lambda_{SOC} (\mathbf{q} \times \mathbf{e}), \quad (4)$$

where β is a proportionality constant that depends on the electronic structure and crystal environment and are similar for the three compounds. To demonstrate and quantify the emergence of an electric polarization we performed *ab initio* calculations in two equivalent magnetic configurations (Fig. 3b) with the same spin rotation vector \mathbf{e} , but with opposite spin propagation vector \mathbf{q} . Therefore, an opposite electric polarization will emerge in each of the configurations. The emergence of the electric polarization in the spin texture is directly obtained by taking the difference between the two equivalent configurations. This procedure provides a direct methodology to extract electric polarization stemming from non-collinear magnetic order⁶⁴. Modifying the q -vector of the spiral, i.e. the size of the supercell, will change the total value of the ferroelectric polarization obtained since it will modify the non-collinear spin order controlling the inverse DM interaction. In our analysis, we use the same spin texture for every chromium trihalide, and hence we can extract the contribution coming from the spin-orbit coupling to the inverse DM interaction.

The emergence of an electric polarization is accompanied by a reconstruction of the electronic density ρ . Therefore, we can analyze the difference in the electronic density $\delta\rho$ between both configurations. This is shown in Fig. 3c for the three chromium halides. We observe that the electronic reconstruction increases by taking a heavier halide. Thus, for the same spin texture, we can see that CrI₃ will produce the strongest ferroelectric polarization. This result is a consequence of the increase of the spin-orbit coupling when one goes down in the halide group, thus demonstrating the effective equations (3) and (4) governed by the SOC prefactor λ_{SOC} .

The reconstruction of the electronic density will lead to the appearance of a ferroelectric force in the atoms in the spin texture in the direction of the emergent electric polarization¹⁰. Therefore, we can compute the force difference between both configurations in Fig. 3b to provide a direct quantification of the electric polarization in CrX₃. Figure 3d shows the force difference between both configurations. We can see that the forces emerge only in the Cr atoms in which the non-collinear magnetism is present. Moreover, we can see that the forces emerge in the z-direction, indicating the direction of the electric dipole, and as expected from the schematic in Fig. 3b. We can quantify the dependence on the halide by taking the average of the force module among Cr-atoms for each of the compounds, as shown in 3d. Taking a heavier

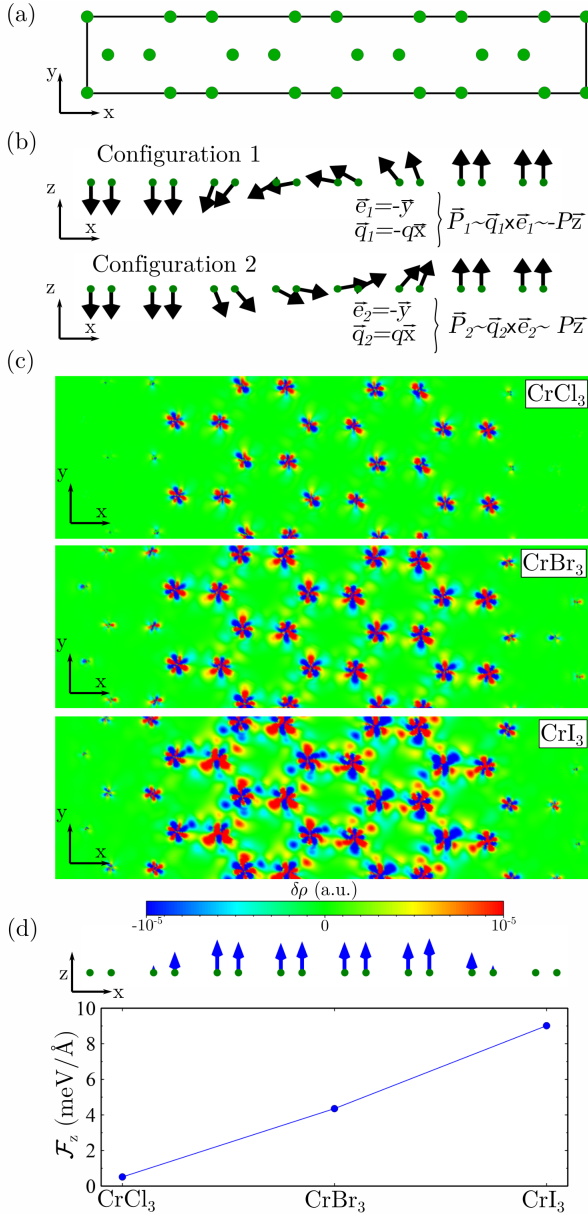


FIG. 3. (a) Unit cell used in the ab initio calculations, Cr atoms depicted in green, halide atoms omitted for clarity. (b) Equivalent non-collinear magnetic configurations with opposite spin propagation vector \mathbf{q} and same helicity \mathbf{e} , and hence opposite electric polarization. (c) Electronic density difference $\delta\rho$ between both equivalent configurations in panel (b) for the three trihalides in the Cr-atoms plane. (d) Force difference between the configurations of the panel (b). A net ferroelectric force emerges in the z -direction in the Cr atoms where the magnetism is non-collinear. An average of the ferroelectric force for each trihalide shows the dependence of the electric polarization with the ligand.

halide produces an increase in the ferroelectric force, as expected from the increase of the spin-orbit coupling. As a reference, NiI₂, a 2D multiferroic governed by this same mechanism of spin-orbit coupling and non-collinear mag-

netism, leads to ferroelectric forces of ≈ 20 meV/ \AA ¹⁰. Therefore, this confirms that spin textures produced in twisted CrX₃ bilayers lead to the emergence of an electric polarization with strong magnetoelectric coupling.

We now elaborate on some conclusions on the strength of multiferroic order in twisted CrX₃ bilayers considering together the results obtained from the low energy model and the ab initio calculations that allowed us to provide a quantification of the inverse DM interaction in these magnetic moiré systems⁶⁵. On the one hand, our ab initio DFT methods show that as the halide becomes heavier, the ferroelectric polarization becomes stronger. On the other hand, the low energy model shows that the anisotropic exchange has a detrimental impact on the formation of the spin texture and hence on the multiferroic order. In particular, in CrI₃ the strong anisotropic exchange might partially quench the formation of a sizable non-collinear magnetic texture. In CrCl₃, the small SOC would yield a comparably weak ferroelectric polarization despite the formation of the non-collinear texture. Therefore, the optimal twisted bilayer that yields the strongest ferroelectric polarization would be CrBr₃, or ultimately, a bilayer of an intermediate stoichiometry between CrBr₃ and CrI₃⁴⁵.

Finally, we analyze the magnetoelectric coupling present in twisted CrX₃ bilayers⁶⁶. To do so, we now include in the low energy Hamiltonian a coupling to an external electric field $\mathbf{E} = (0, 0, E_z)$ perpendicular to the twisted system in the z -direction

$$\mathcal{H}_E = \frac{1}{2} \sum_{ij} \mathbf{E} \cdot \mathbf{P}_{ij}. \quad (5)$$

We now show how this interlayer bias allows controlling the magnetic order due to the emergent multiferroicity⁶⁷. Figures 4a and 4b show the spin texture and the associated electric polarization at $E_z/J = 3$. We can observe that the ground state spin texture shown in Fig. 2a gets significantly modified due to the strong magnetoelectric coupling, leading to the formation of a magnetic skyrmion around the AA rhombohedral stacking in one of the layers^{38,39,68–74}. Interestingly, such a magnetic state features a non-zero total electric polarization in the z -direction. The evolution of the total electric polarization in the moiré supercell in the z -direction as a function of the external electric field is shown in Fig. 4c. The different bumps in P_z as a function of the electric field indicate transitions to different non-trivial spin textures which are shown as insets in Fig. 4c. Starting at $E_z/J = 0$ in the ground state spin texture, at $E_z/J = \pm 3$ the magnetic skyrmion shown in Fig. 4ab arises. At $E_z/J = \pm 5$ a second pair of magnetic skyrmions emerge in the other layer around the AB/BA stacking regions⁷⁵. The critical electric field required to produce a transition to the skyrmionic phase is inversely proportional to the strength of the λ_{SOC} . As a reference, $J \approx 3$ meV and $\alpha\lambda_{SOC} \approx 10^{-4}\text{e}$ (e electron charge) in twisted CrBr₃ bilayers, implying that such magnetic transitions can be

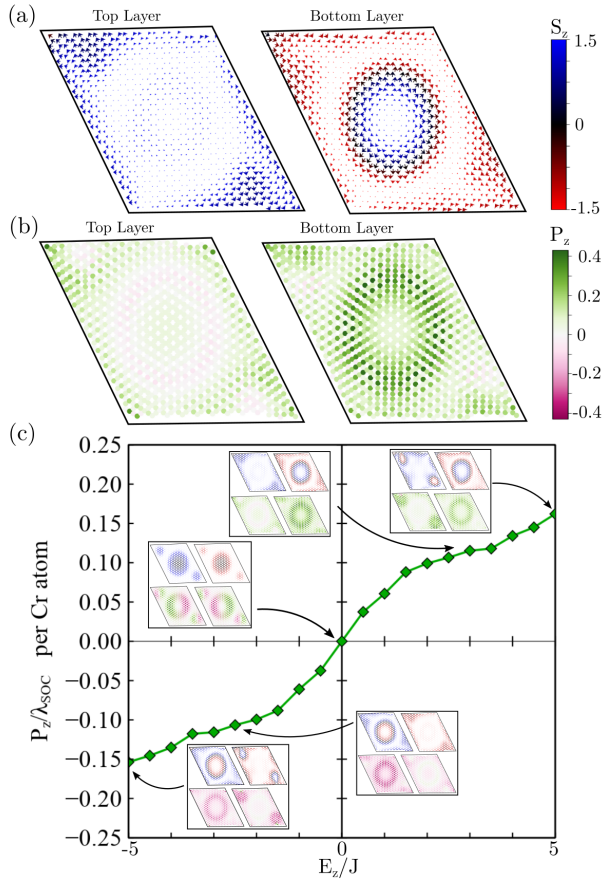


FIG. 4. (a) Spin texture in moiré unit cell at $E_z/J = 3$, a magnetic skyrmion emerges in the bottom layer. (b) Associated electric polarization to the spin texture. (c) Evolution of the net electric polarization in the z-direction P_z as a function of the electric field. Different spin textures appear as a function of the electric field: ground state spin texture at $E_z/J = 0$, a magnetic skyrmion appears in the AA stacking area in one of the layers at $E_z/J = \pm 3$, and a second pair of magnetic skyrmions emerge in the other layer around the AB/BA stacking regions at $E_z/J = \pm 5$.

experimentally driven via gating at voltages of $1 - 10$ V⁶⁷. This brings twisted CrBr₃ bilayers as a promising platform for the electric control of non-trivial magnetic textures, and ultimately as a platform for magnetoelectric skyrmionics.

III. CONCLUSIONS

To summarize, we have demonstrated that twisted CrX₃ bilayers develop a multiferroic order due to the interplay between the moiré structure, non-collinear magnetic order, and spin-orbit coupling. We have provided a quantification of the strength of the multiferroic order for this family of compounds, finding that, among the stoichiometric chromium trihalides, CrBr₃ is expected to display the strongest multiferroic and magnetoelectric coupling. Furthermore, we have shown that this strong magnetoelectric coupling allows an electrical control of non-trivial magnetic textures using an interlayer bias. Our results put forward a strategy to design a new family of artificial multiferroics with a strong magnetoelectric coupling based on twisted magnetic van der Waals materials.

DATA AVAILABILITY STATEMENT

All data that support the findings of this study are included within the article (and any supplementary files).

ACKNOWLEDGEMENTS

We acknowledge the computational resources provided by the Aalto Science-IT project, and the financial support from the Academy of Finland Projects No. 331342, No. 336243 and No. 349696 and the Jane and Aatos Erkko Foundation. We thank P. Liljeroth for useful discussions.

¹ Nicola A. Hill, “Why are there so few magnetic ferroelectrics?” *The Journal of Physical Chemistry B* **104**, 6694–6709 (2000).

² N. A. Spaldin and R. Ramesh, “Advances in magnetoelectric multiferroics,” *Nature Materials* **18**, 203–212 (2019).

³ Manfred Fiebig, Thomas Lottermoser, Dennis Meier, and Morgan Trassin, “The evolution of multiferroics,” *Nature Reviews Materials* **1** (2016), 10.1038/natrevmats.2016.46.

⁴ Manfred Fiebig, “Revival of the magnetoelectric effect,” *Journal of Physics D: Applied Physics* **38**, R123–R152 (2005).

⁵ T. Kimura, T. Goto, H. Shintani, K. Ishizaka, T. Arima, and Y. Tokura, “Magnetic control of ferroelectric polarization,” *Nature* **426**, 55–58 (2003).

⁶ N. Hur, S. Park, P. A. Sharma, J. S. Ahn, S. Guha, and S.-W. Cheong, “Electric polarization reversal and memory in

a multiferroic material induced by magnetic fields,” *Nature* **429**, 392–395 (2004).

⁷ Martin Gajek, Manuel Bibes, Stéphane Fusil, Karim Bouzehouane, Josep Fontcuberta, Agnès Barthélémy, and Albert Fert, “Tunnel junctions with multiferroic barriers,” *Nature Materials* **6**, 296–302 (2007).

⁸ Ce-Wen Nan, M. I. Bichurin, Shuxiang Dong, D. Viehland, and G. Srinivasan, “Multiferroic magnetoelectric composites: Historical perspective, status, and future directions,” *Journal of Applied Physics* **103**, 031101 (2008).

⁹ D. Pantel, S. Goetze, D. Hesse, and M. Alexe, “Reversible electrical switching of spin polarization in multiferroic tunnel junctions,” *Nature Materials* **11**, 289–293 (2012).

¹⁰ Adolfo O Fumega and J L Lado, “Microscopic origin of multiferroic order in monolayer NiI₂,” *2D Materials* **9**, 025010 (2022).

- ¹¹ Qian Song, Connor A. Occhialini, Emre Ergeçen, Batyr Ilyas, Danila Amoroso, Paolo Barone, Jesse Kapeghian, Kenji Watanabe, Takashi Taniguchi, Antia S. Botana, Silvia Picozzi, Nuh Gedik, and Riccardo Comin, "Evidence for a single-layer van der waals multiferroic," *Nature* **602**, 601–605 (2022).
- ¹² Yurong Su, Xinlu Li, Meng Zhu, Jia Zhang, Long You, and Evgeny Y. Tsymbal, "Van der waals multiferroic tunnel junctions," *Nano Letters* **21**, 175–181 (2020).
- ¹³ M. Serlin, C. L. Tschirhart, H. Polshyn, Y. Zhang, J. Zhu, K. Watanabe, T. Taniguchi, L. Balents, and A. F. Young, "Intrinsic quantized anomalous hall effect in a moiré heterostructure," *Science* **367**, 900–903 (2020).
- ¹⁴ Fabian R. Geisenhof, Felix Winterer, Anna M. Seiler, Jakob Lenz, Tianyi Xu, Fan Zhang, and R. Thomas Weitz, "Quantum anomalous hall octet driven by orbital magnetism in bilayer graphene," *Nature* **598**, 53–58 (2021).
- ¹⁵ Tingxin Li, Shengwei Jiang, Bowen Shen, Yang Zhang, Lihong Li, Zui Tao, Trithep Devakul, Kenji Watanabe, Takashi Taniguchi, Liang Fu, Jie Shan, and Kin Fai Mak, "Quantum anomalous hall effect from intertwined moiré bands," *Nature* **600**, 641–646 (2021).
- ¹⁶ Kevin P. Nuckolls, Myungchul Oh, Dillon Wong, Biao Lian, Kenji Watanabe, Takashi Taniguchi, B. Andrei Bernevig, and Ali Yazdani, "Strongly correlated chern insulators in magic-angle twisted bilayer graphene," *Nature* **588**, 610–615 (2020).
- ¹⁷ Yuan Cao, Valla Fatemi, Shiang Fang, Kenji Watanabe, Takashi Taniguchi, Efthimios Kaxiras, and Pablo Jarillo-Herrero, "Unconventional superconductivity in magic-angle graphene superlattices," *Nature* **556**, 43–50 (2018).
- ¹⁸ Myungchul Oh, Kevin P. Nuckolls, Dillon Wong, Ryan L. Lee, Xiaomeng Liu, Kenji Watanabe, Takashi Taniguchi, and Ali Yazdani, "Evidence for unconventional superconductivity in twisted bilayer graphene," *Nature* **600**, 240–245 (2021).
- ¹⁹ Shawlienu Kezilebieke, Md Nurul Huda, Viliam Vaňo, Markus Aapro, Somesh C. Ganguli, Orlando J. Silveira, Szczepan Głodzik, Adam S. Foster, Teemu Ojanen, and Peter Liljeroth, "Topological superconductivity in a van der waals heterostructure," *Nature* **588**, 424–428 (2020).
- ²⁰ Shawlienu Kezilebieke, Viliam Vaňo, Md N. Huda, Markus Aapro, Somesh C. Ganguli, Peter Liljeroth, and Jose L. Lado, "Moiré-enabled topological superconductivity," *Nano Letters* **22**, 328–333 (2022).
- ²¹ Jeong Min Park, Yuan Cao, Kenji Watanabe, Takashi Taniguchi, and Pablo Jarillo-Herrero, "Tunable strongly coupled superconductivity in magic-angle twisted trilayer graphene," *Nature* **590**, 249–255 (2021).
- ²² Hyunjin Kim, Youngjoon Choi, Cyprian Lewandowski, Alex Thomson, Yiran Zhang, Robert Polski, Kenji Watanabe, Takashi Taniguchi, Jason Alicea, and Stevan Nadj-Perge, "Evidence for unconventional superconductivity in twisted trilayer graphene," *Nature* **606**, 494–500 (2022).
- ²³ Viliam Vaňo, Mohammad Amini, Somesh C. Ganguli, Guangze Chen, Jose L. Lado, Shawlienu Kezilebieke, and Peter Liljeroth, "Artificial heavy fermions in a van der waals heterostructure," *Nature* **599**, 582–586 (2021).
- ²⁴ Shiwei Shen, Chenhaoping Wen, Pengfei Kong, Jingjing Gao, Jianguo Si, Xuan Luo, Wenjian Lu, Yuping Sun, Gang Chen, and Shichao Yan, "Inducing and tuning kondo screening in a narrow-electronic-band system," *Nature Communications* **13** (2022), 10.1038/s41467-022-29891-4.
- ²⁵ Wei Ruan, Yi Chen, Shujie Tang, Jinwoong Hwang, Hsin-Zon Tsai, Ryan L. Lee, Meng Wu, Hyejin Ryu, Salman Kahn, Franklin Liou, Caihong Jia, Andrew Aikawa, Choongyu Hwang, Feng Wang, Yongseong Choi, Steven G. Louie, Patrick A. Lee, Zhi-Xun Shen, Sung-Kwan Mo, and Michael F. Crommie, "Evidence for quantum spin liquid behaviour in single-layer 1t-TaSe₂ from scanning tunnelling microscopy," *Nature Physics* **17**, 1154–1161 (2021).
- ²⁶ Miguel M. Ugeda, Aaron J. Bradley, Yi Zhang, Seita Onishi, Yi Chen, Wei Ruan, Claudia Ojeda-Aristizabal, Hyejin Ryu, Mark T. Edmonds, Hsin-Zon Tsai, and et al., "Characterization of collective ground states in single-layer nbse₂," *Nature Physics* **12**, 92–97 (2015).
- ²⁷ Bevin Huang, Genevieve Clark, Efrén Navarro-Moratalla, Dahlia R. Klein, Ran Cheng, Kyle L. Seyler, Ding Zhong, Emma Schmidgall, Michael A. McGuire, David H. Cobden, Wang Yao, Di Xiao, Pablo Jarillo-Herrero, and Xiaodong Xu, "Layer-dependent ferromagnetism in a van der waals crystal down to the monolayer limit," *Nature* **546**, 270–273 (2017).
- ²⁸ Shuguo Yuan, Xin Luo, Hung Lit Chan, Chengcheng Xiao, Yawei Dai, Maohai Xie, and Jianhua Hao, "Room-temperature ferroelectricity in mott2 down to the atomic monolayer limit," *Nature Communications* **10**, 1775 (2019).
- ²⁹ Yuan Cao, Valla Fatemi, Ahmet Demir, Shiang Fang, Spencer L. Tomarken, Jason Y. Luo, Javier D. Sanchez-Yamagishi, Kenji Watanabe, Takashi Taniguchi, Efthimios Kaxiras, Ray C. Ashoori, and Pablo Jarillo-Herrero, "Correlated insulator behaviour at half-filling in magic-angle graphene superlattices," *Nature* **556**, 80–84 (2018).
- ³⁰ Xiaobo Lu, Petr Stepanov, Wei Yang, Ming Xie, Mohammed Ali Aamir, Ipsita Das, Carles Urgell, Kenji Watanabe, Takashi Taniguchi, Guangyu Zhang, Adrian Bachtold, Allan H. MacDonald, and Dmitri K. Efetov, "Superconductors, orbital magnets and correlated states in magic-angle bilayer graphene," *Nature* **574**, 653–657 (2019).
- ³¹ H. Polshyn, J. Zhu, M. A. Kumar, Y. Zhang, F. Yang, C. L. Tschirhart, M. Serlin, K. Watanabe, T. Taniguchi, A. H. MacDonald, and A. F. Young, "Electrical switching of magnetic order in an orbital chern insulator," *Nature* **588**, 66–70 (2020).
- ³² Fengcheng Wu, Timothy Lovorn, Emanuel Tutuc, Ivar Martin, and A. H. MacDonald, "Topological insulators in twisted transition metal dichalcogenide homobilayers," *Phys. Rev. Lett.* **122**, 086402 (2019).
- ³³ Mikael Haavisto, J. L. Lado, and Adolfo Otero Fumega, "Topological multiferroic order in twisted transition metal dichalcogenide bilayers," *SciPost Phys.* **13**, 052 (2022).
- ³⁴ Tiancheng Song, Qi-Chao Sun, Eric Anderson, Chong Wang, Jimin Qian, Takashi Taniguchi, Kenji Watanabe, Michael A. McGuire, Rainer Stöhr, Di Xiao, Ting Cao, Jörg Wrachtrup, and Xiaodong Xu, "Direct visualization of magnetic domains and moiré magnetism in twisted 2d magnets," *Science* **374**, 1140–1144 (2021).
- ³⁵ Chong Wang, Yuan Gao, Hongyan Lv, Xiaodong Xu, and Di Xiao, "Stacking domain wall magnons in twisted van der waals magnets," *Phys. Rev. Lett.* **125**, 247201 (2020).
- ³⁶ Hongchao Xie, Xiangpeng Luo, Gaihua Ye, Zhipeng Ye, Haiwen Ge, Suk Hyun Sung, Emily Rennich, Shaohua Yan, Yang Fu, Shangjie Tian, Hechang Lei, Robert Hovden, Kai Sun, Rui He, and Liuyan Zhao, "Twist engineering of the two-dimensional magnetism in double bilayer

- chromium triiodide homostructures,” *Nature Physics* **18**, 30–36 (2021).
- ³⁷ Yang Xu, Ariana Ray, Yu-Tsun Shao, Shengwei Jiang, Kihong Lee, Daniel Weber, Joshua E. Goldberger, Kenji Watanabe, Takashi Taniguchi, David A. Muller, Kin Fai Mak, and Jie Shan, “Coexisting ferromagnetic–antiferromagnetic state in twisted bilayer CrI₃,” *Nature Nanotechnology* **17**, 143–147 (2021).
- ³⁸ Feiping Xiao, Keqiu Chen, and Qingjun Tong, “Magnetization textures in twisted bilayer crx₃ (x=br, i),” *Phys. Rev. Research* **3**, 013027 (2021).
- ³⁹ Muhammad Akram, Harrison LaBollita, Dibyendu Dey, Jesse Kapeghian, Onur Erten, and Antia S. Botana, “Moiré skyrmions and chiral magnetic phases in twisted CrX₃ (x = i, br, and cl) bilayers,” *Nano Letters* **21**, 6633–6639 (2021).
- ⁴⁰ Yang Xu, Ariana Ray, Yu-Tsun Shao, Shengwei Jiang, Daniel Weber, Joshua E. Goldberger, Kenji Watanabe, Takashi Taniguchi, David A. Muller, Kin Fai Mak, and Jie Shan, “Emergence of a noncollinear magnetic state in twisted bilayer CrI₃,” arXiv e-prints , arXiv:2103.09850 (2021), arXiv:2103.09850 [cond-mat.mtrl-sci].
- ⁴¹ Hongchao Xie, Xiangpeng Luo, Zhipeng Ye, Gaihua Ye, Haiwen Ge, Shaohua Yan, Yang Fu, Shangjie Tian, Hechang Lei, Kai Sun, Rui He, and Liuyan Zhao, “Evidence of Noncollinear Spin Texture in Magnetic Moiré Superlattices,” arXiv e-prints , arXiv:2204.01636 (2022), arXiv:2204.01636 [cond-mat.mtrl-sci].
- ⁴² J L Lado and J Fernández-Rossier, “On the origin of magnetic anisotropy in two dimensional CrI₃,” *2D Materials* **4**, 035002 (2017).
- ⁴³ Wei-Bing Zhang, Qian Qu, Peng Zhu, and Chi-Hang Lam, “Robust intrinsic ferromagnetism and half semiconductivity in stable two-dimensional single-layer chromium trihalides,” *Journal of Materials Chemistry C* **3**, 12457–12468 (2015).
- ⁴⁴ Kok Wee Song and Vladimir I. Fal’ko, “Superexchange and spin-orbit coupling in monolayer and bilayer chromium trihalides,” *Phys. Rev. B* **106**, 245111 (2022).
- ⁴⁵ Thomas A. Tartaglia, Joseph N. Tang, Jose L. Lado, Faranak Bahrami, Mykola Abramchuk, Gregory T. McCandless, Meaghan C. Doyle, Kenneth S. Burch, Ying Ran, Julia Y. Chan, and Fazel Tafti, “Accessing new magnetic regimes by tuning the ligand spin-orbit coupling in van der waals magnets,” *Science Advances* **6** (2020), 10.1126/sciadv.abb9379.
- ⁴⁶ Lucas Webster and Jia-An Yan, “Strain-tunable magnetic anisotropy in monolayer crcl₃, crbr₃, and cri₃,” *Phys. Rev. B* **98**, 144411 (2018).
- ⁴⁷ In the absence of strain, CrCl₃ shows in-plane anisotropy.
- ⁴⁸ Changsong Xu, Junsheng Feng, Hongjun Xiang, and Laurent Bellaiche, “Interplay between kitaev interaction and single ion anisotropy in ferromagnetic CrI₃ and CrGeTe₃ monolayers,” *npj Computational Materials* **4** (2018), 10.1038/s41524-018-0115-6.
- ⁴⁹ Alexey Kartsev, Mathias Augustin, Richard F. L. Evans, Kostya S. Novoselov, and Elton J. G. Santos, “Biquadratic exchange interactions in two-dimensional magnets,” *npj Computational Materials* **6** (2020), 10.1038/s41524-020-00416-1.
- ⁵⁰ Lebing Chen, Jae-Ho Chung, Bin Gao, Tong Chen, Matthew B. Stone, Alexander I. Kolesnikov, Qingzhen Huang, and Pengcheng Dai, “Topological spin excitations in honeycomb ferromagnet cri₃,” *Phys. Rev. X* **8**, 041028 (2018).
- ⁵¹ Xiaobo Lu, Ruixiang Fei, Linghan Zhu, and Li Yang, “Meron-like topological spin defects in monolayer CrCl₃,” *Nature Communications* **11** (2020), 10.1038/s41467-020-18573-8.
- ⁵² Nikhil Sivadas, Satoshi Okamoto, Xiaodong Xu, Craig. J. Fennie, and Di Xiao, “Stacking-dependent magnetism in bilayer CrI₃,” *Nano Letters* **18**, 7658–7664 (2018).
- ⁵³ D. Soriano, C. Cardoso, and J. Fernández-Rossier, “Interplay between interlayer exchange and stacking in CrI₃ bilayers,” *Solid State Communications* **299**, 113662 (2019).
- ⁵⁴ Weijong Chen, Zeyuan Sun, Zhongjie Wang, Lehua Gu, Xiaodong Xu, Shiwei Wu, and Chunlei Gao, “Direct observation of van der waals stacking-dependent interlayer magnetism,” *Science* **366**, 983–987 (2019).
- ⁵⁵ Marco Gibertini, “Magnetism and stability of all primitive stacking patterns in bilayer chromium trihalides,” *Journal of Physics D: Applied Physics* **54**, 064002 (2020).
- ⁵⁶ David Soriano, “Domain wall formation and magnon localization in twisted chromium trihalides,” *physica status solidi (RRL) – Rapid Research Letters* **16**, 2200078 (2022).
- ⁵⁷ In the case of CrCl₃ the stacking dependence of the interlayer magnetic exchange has not been fully established. Ab initio calculations have found a highly functional dependence on the interlayer magnetic exchange^{39,76}. However, it has also been shown, that this interlayer coupling is weak and external fields, can drive bilayer CrCl₃ to the same scenario as the other two halides⁷⁶.
- ⁵⁸ A detailed explanation of the interlayer exchange parametrization and the robustness of the results against perturbations to it, such as the twist angle, are included in the Supplemental Material.
- ⁵⁹ Computational details about the minimization procedure to obtain the ground state are included in the Supplemental Material.
- ⁶⁰ Hosho Katsura, Naoto Nagaosa, and Alexander V. Balatsky, “Spin current and magnetoelectric effect in non-collinear magnets,” *Phys. Rev. Lett.* **95**, 057205 (2005).
- ⁶¹ Maxim Mostovoy, “Ferroelectricity in spiral magnets,” *Phys. Rev. Lett.* **96**, 067601 (2006).
- ⁶² P. Hohenberg and W. Kohn, “Inhomogeneous electron gas,” *Phys. Rev.* **136**, B864–B871 (1964).
- ⁶³ An in-plane spin texture provides results on the same order of magnitude for CrCl₃.
- ⁶⁴ A detailed explanation about the DFT calculations can be found in the Supplemental Material.
- ⁶⁵ See the Supplemental material for a more detailed description of how these conclusions are derived.
- ⁶⁶ Importantly, to drive conclusions about the strength of the magnetoelectric coupling we are considering the parameters corresponding to CrBr₃, which is found to display the strongest multiferroic order.
- ⁶⁷ Guanghui Cheng, Mohammad Mushfiqur Rahman, Andres Llacsahuanga Allcca, Avinash Rustagi, Xingtao Liu, Lina Liu, Lei Fu, Yanglin Zhu, Zhiqiang Mao, Kenji Watanabe, Takashi Taniguchi, Pramey Upadhyaya, and Yong P. Chen, “Electrically tunable moiré magnetism in twisted double bilayer antiferromagnets,” arXiv e-prints , arXiv:2204.03837 (2022), arXiv:2204.03837 [cond-mat.mtrl-sci].
- ⁶⁸ Qingjun Tong, Fei Liu, Jiang Xiao, and Wang Yao, “Skyrmions in the moiré of van der waals 2d magnets,” *Nano Letters* **18**, 7194–7199 (2018).

- ⁶⁹ Sujay Ray and Tanmoy Das, “Hierarchy of multi-order skyrmion phases in twisted magnetic bilayers,” Phys. Rev. B **104**, 014410 (2021).
- ⁷⁰ Kasra Hejazi, Zhu-Xi Luo, and Leon Balents, “Heterobilayer moiré magnets: Moiré skyrmions and commensurate-incommensurate transitions,” Phys. Rev. B **104**, L100406 (2021).
- ⁷¹ Kasra Hejazi, Zhu-Xi Luo, and Leon Balents, “Non-collinear phases in moiré magnets,” Proceedings of the National Academy of Sciences **117**, 10721–10726 (2020).
- ⁷² Yingying Wu, Brian Francisco, Zhijie Chen, Wei Wang, Yu Zhang, Caihua Wan, Xiufeng Han, Hang Chi, Yasen Hou, Alessandro Lodesani, Gen Yin, Kai Liu, Yong tao Cui, Kang L. Wang, and Jagadeesh S. Moodera, “A van der waals interface hosting two groups of magnetic skyrmions,” Advanced Materials **34**, 2110583 (2022).
- ⁷³ Fawei Zheng, “Magnetic skyrmion lattices in a novel 2d-twisted bilayer magnet,” Advanced Functional Materials **33**, 2206923 (2023).
- ⁷⁴ Kyoung-Min Kim, Do Hoon Kiem, Grigory Bednik, Myung Joon Han, and Moon Jip Park, “Theory of Moire Magnets and Topological Magnons: Applications to Twisted Bilayer CrI₃,” arXiv e-prints , arXiv:2206.05264 (2022), arXiv:2206.05264 [cond-mat.str-el].
- ⁷⁵ See Supplemental material for a discussion on topological magnetoelectric couplings associated to skyrmions.
- ⁷⁶ Dahlia R. Klein, David MacNeill, Qian Song, Daniel T. Larson, Shiang Fang, Mingyu Xu, R. A. Ribeiro, P. C. Canfield, Efthimios Kaxiras, Riccardo Comin, and Pablo Jarillo-Herrero, “Enhancement of interlayer exchange in an ultrathin two-dimensional magnet,” Nature Physics **15**, 1255–1260 (2019).